A Mathieu function boundary spectral method for acoustic scattering

Matthew Colbrook
University of Cambridge

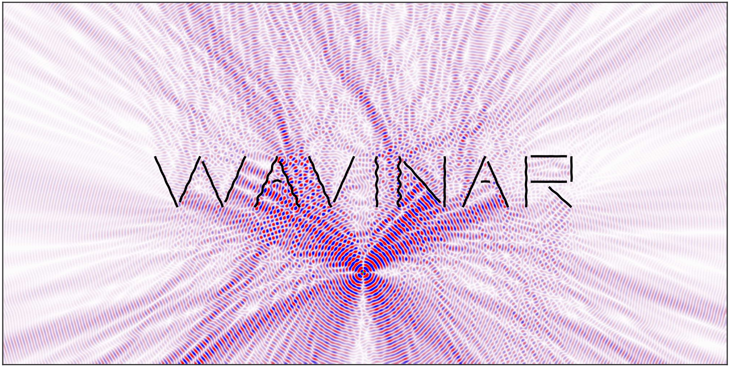

Example elastic plates produced for Wavinar seminar series:
https://www.icms.org.uk/V_Wavinar.php

Collaborators for papers in this talk

Lorna Ayton (Cambridge)	Paruchuri Chaitanya (Southampton)	Thomas Geyer (Brandenburg)	Alistair Hales (Cambridge)
			

Anastasia Kisil (Manchester)	Matthew Priddin (Cambridge)	Ennes Sarradj (TU Berlin)
		

With special thanks also to Justin Jaworski (the owl guru) at Lehigh for numerous discussions on the physical models.

Sketch of talk

Goal: Numerically solve scattering problems in applications with complicated BCs. Want: **accurate**, **fast**, **flexible** (+ **easy-to-use**?).

Outline (3 fun examples):

- Building a numerical method
- BC I: Porosity (variable Robin)
- Application I: Silent flight of owls
- BC II: Elasticity (4th order coupled ODE)
- Application II: Acoustic black holes
- BC III: Forchheimer (nonlinear inertial correction)
- Application III: Porous foam aerofoils without turbulent simulations
- Conclusions and future work

Scattering problem

Acoustic 2D scattering governed by the Helmholtz equation

$$\frac{\partial^2 \phi}{\partial x^2} + \frac{\partial^2 \phi}{\partial y^2} + k_0^2 \phi = 0, \quad (x, y) \in \mathcal{D}.$$

Focus on $\partial\mathcal{D} = \{(x, 0) : x \in [-1, 1]\}$.
Sommerfeld radiation condition at infinity (radiates <u>to</u> infinity):

$$\lim_{r \to \infty} r^{\frac{1}{2}} \left(\frac{\partial}{\partial r} - ik_0 \right) \phi(r, \theta) = 0.$$

NB: Multiple (non-touching) plates dealt with similarly.

Simple idea: Separation of variables

Elliptic coordinates $x = \cosh(\nu)\cos(\tau), y = \sinh(\nu)\sin(\tau)$

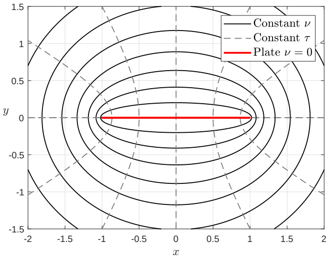

$\Rightarrow$

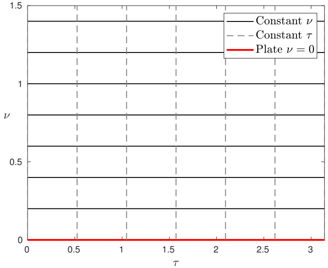

$$\phi(\nu, \tau) = \sum_{m=1}^{\infty} a_m \mathrm{se}_m(\tau)\mathrm{Hse}_m(\nu).$$

Will determine the unknown coefficients using collocation.

Angular Mathieu functions

Expand in a rapidly convergent sine series:

$$\mathrm{se}_m(Q;\tau) = \mathrm{se}_m(\tau) = \sum_{l=1}^{\infty} B_l^{(m)} \sin(l\tau), \quad Q = k_0^2/4.$$

For even order solutions, eigenvalue problem becomes

$$\begin{pmatrix} 2^2 - \lambda_{2m} & Q & & & \\ Q & 4^2 - \lambda_{2m} & Q & & \\ & Q & 6^2 - \lambda_{2m} & Q & \\ & & \ddots & \ddots & \ddots \end{pmatrix} \begin{pmatrix} B_2^{(2m)} \\ B_4^{(2m)} \\ B_6^{(2m)} \\ \vdots \end{pmatrix} = 0.$$

Similar system for odd order solutions.

Radial Mathieu functions

Expand in a rapidly convergent Bessel function series:

$$\mathrm{Hse}_m(\nu) = \sum_{l=1}^{\infty} \frac{(-1)^{l+m} B_l^{(m)}}{C_m} \Big[J_{l-1}(\mathrm{e}^{-\nu}\sqrt{Q}) H^{(1)}_{l+p_m}(\mathrm{e}^{\nu}\sqrt{Q}) \\ - J_{l+p_m}(\mathrm{e}^{-\nu}\sqrt{Q}) H^{(1)}_{l-1}(\mathrm{e}^{\nu}\sqrt{Q}) \Big],$$

where $p_m = 1$ if m is even and $p_m = 0$ if m is odd.

(Convention: C_m such that $\mathrm{Hse}'_m(0) = 1$.)

Warning: Care needed in some regimes to avoid underflow and overflow associated with cancellations between the Bessel and Hankel functions. Solve this using asymptotics (details in C. & Kisil 2020).

Bottom line: With a bit of care, both types of Mathieu functions can be accurately and efficiently evaluated $\Rightarrow$ can be used with collocation.

Singular integral equation interpretation

Green's function that vanishes on the horizontal axis

$$G(x, y; \tilde{x}, \tilde{y}) = \frac{H_0^{(1)}(k_0\sqrt{(x-\tilde{x})^2 + (y-\tilde{y})^2}) - H_0^{(1)}(k_0\sqrt{(x-\tilde{x})^2 + (y+\tilde{y})^2})}{4i}.$$

We get an explicit diagonalisation for $x \in [-1, 1]$:

$$\frac{\partial}{\partial y}\int_{-1}^{1} \mathrm{se}_m(\cos^{-1}(\tilde{x}))\partial_{\tilde{y}} G(x, 0; \tilde{x}, 0)d\tilde{x} = \frac{d_m}{\sin(\cos^{-1}(x))}\mathrm{se}_m(\cos^{-1}(x)).$$

Examples in this talk can be recast in terms of this double-layer potential.

We can now build a collocation method!

BC I: Porosity (variable Robin)

Incident field with velocity potential ϕ_{I}. Impedance BC:

$$\frac{\partial \phi}{\partial y}\Big|_{y=0}(x) + \frac{\partial \phi_{\mathrm{I}}}{\partial y}\Big|_{y=0}(x) = \mu(x)[\phi](x), \quad x \in [-1, 1].$$

Truncate expansion to N terms, the integral equation becomes

$$\sum_{n=1}^{N} a_n \mathrm{se}_n\left(\cos^{-1}(x)\right)\left[1 - 2\mathrm{Hse}_n(0)\mu(x)\sqrt{1-x^2}\right] = -\sqrt{1-x^2} \cdot \frac{\partial \phi_{\mathrm{I}}}{\partial y}(x).$$

Collocate at N Cheb. pts (NB: reformulate as diagonal system if $\mu = 0$).

NB: Gain sine series for far-field directivity, $D(\theta)$, defined via

$$\phi(r, \theta) \sim D(\theta)\frac{\mathrm{e}^{\mathrm{i}wr}}{\sqrt{r}}, \quad \text{as} \quad r \to \infty.$$

Total far-field noise, measured in dB:

$$P = 10 \log_{10}\left(\int_0^{\pi} |D(\theta)|^2 d\theta\right).$$

Application I: Silent flight of owls

Porosity promotes the silent flight of owls?

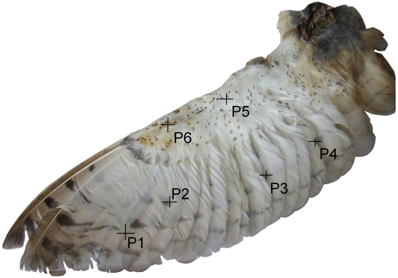

Wing measurements $\Rightarrow \mu$.
Owl vs. buzzard in [Ayton, C., Geyer, Chaitanya & Sarradj 2020].
First study of variable porosity parameter.
Goal: porosity adapted aerofoils for noise reduction

Application I: Silent flight of owls

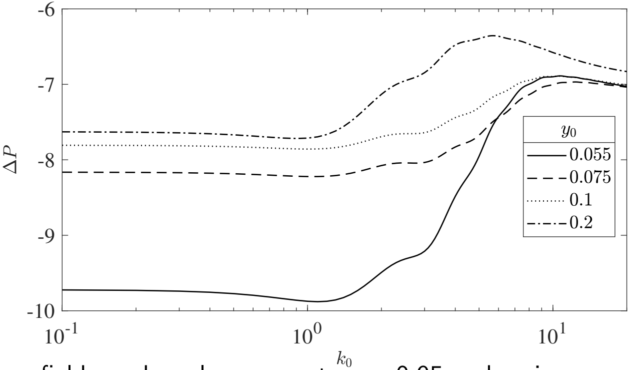

ΔP for a near-field quadrupole source at $x_0 = 0.95$ and various y_0. Negative values indicate the owl is quieter than the buzzard by that many dB.

Further findings:

- Leading-edge noise also reduced for owl (despite similar μ there).
- Porosity decreasing from trailing edge to leading edge can be quieter than constant porosity (variably porous plate can induce a destructively interfering leading-edge field)

Application I: Silent flight of owls

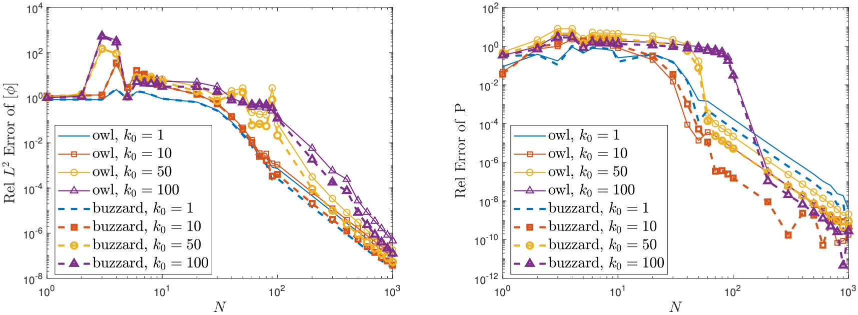

Relative errors for $[\phi]$ (left, L^2 norm error over $[-1, 1]$) and P (right).

BC II: Elasticity (4th order coupled ODE)

Porous plate with evenly-spaced circular apertures of radius R and fractional open area α_H. Plate deformation $\eta(x)$ satisfies:

$$B_0(x)\eta(x) + \sum_{l=1}^{4} B_l(x)\frac{\partial^l \eta}{\partial x^l}(x) = -\rho_f c_0^2 \left(1 + \frac{4\alpha_H}{\pi}\right)[\phi](x).$$

Kinematic condition for incident field ϕ_{I}:

$$\frac{\partial \phi}{\partial y}\Big|_{y=0}(x) + \frac{\partial \phi_{\mathrm{I}}}{\partial y}\Big|_{y=0}(x) = k_0^2\Big[(1-\alpha_H)\eta(x) + \alpha_H \eta_a(x)\Big].$$

$\eta_a = 2[\phi]/(\pi k_0^2 R) =$ average fluid displacement in apertures.

Endpoint ± 1 either free $\eta'' = \eta''' = 0$ or clamped $\eta = \eta' = 0$.

BC II: Elasticity (4th order coupled ODE)

Expansion of η in Chebyshev polynomials

$$\eta(x) = \sum_{j=0}^{N-1} b_j T_j(x).$$

Collocate thin plate equation at $N-4$ Chebyshev points

$$\sum_{j=0}^{N-1} \frac{b_j \pi}{2\rho_f c_0^2} \sum_{l=0}^{4} B_l(x) T_j^{(l)}(x) + (\pi + 4\alpha_H) \sum_{m=1}^{M} a_m \mathrm{se}_m \left(\cos^{-1}(x)\right) \mathrm{Hse}_m(0) = 0.$$

Collocate kinematic relation at M Chebyshev points

$$\sqrt{1-x^2} \cdot \frac{\partial \phi_{\mathrm{I}}}{\partial y}(x) + \sum_{m=1}^{M} a_m \mathrm{se}_m \left(\cos^{-1}(x)\right) \left[1 - \frac{4\alpha_H \mathrm{Hse}_m(0)}{\pi R} \sqrt{1-x^2}\right]$$

$$= k_0^2 (1-\alpha_H) \sqrt{1-x^2} \sum_{j=0}^{N-1} b_j T_j(x).$$

$+$ 4 relations for η BCs $\Rightarrow (M+N) \times (M+N)$ system for coefficients.

Application II: Acoustic black holes

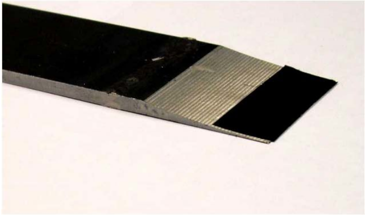

Aluminium plate of thickness $h(x)$ with

$$B(x) = \frac{Eh(x)^3}{12(1-\nu^2)}, \quad E = 69 \times 10^9 \mathrm{Pa}, \quad \nu = 0.35$$

$$\frac{d^2}{dx^2}\left(B(x)\eta''(x)\right) - m_0 h(x)\eta(x) = -\rho_f c_0^2 \left(1 + \frac{4\alpha_H}{\pi}\right)[\phi](x)$$

First study of interaction of acoustic blackholes with incident field.
Goal: can acoustic blackholes absorb most of incident field?

Incident plane wave, $k_0 = 20$, $h(x) = 0.001x^2 + h_0$

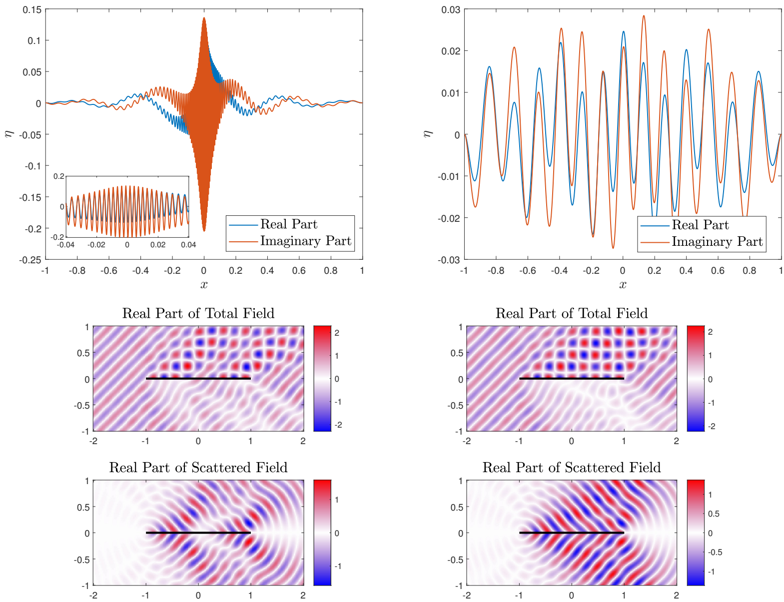

Left: $h_0 = 10^{-6}$. Right: $h_0 = 10^{-3}$.

Typical convergence behaviour

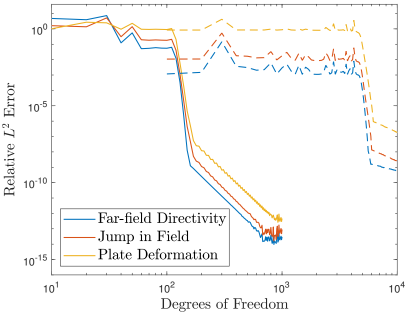

Incident plane wave for $h_0 = 10^{-6}$ (dashed) and $h_0 = 10^{-3}$ (full).

Several digits of rel. accuracy, even for (nearly) singular elastic BCs!

BC III: Forchheimer (nonlin. inertial correction for large Re)

$$\left.\frac{\partial \phi}{\partial y}\right|_{y=0}(x) + \left.\frac{\partial \phi_{\mathrm{I}}}{\partial y}\right|_{y=0}(x) = C_0(x)\eta_a|_{y=0}, \quad x \in [-1, 1].$$

Nonlinear correction important for foam-like materials:

$$[\phi] = C_1(x)\eta_a + C_2(x)\eta_a|\eta_a|, \quad x \in [-1, 1].$$

C_1, C_2 defined in terms of physical parameters. Expand η_a via

$$\eta_a(x) = \sum_{j=0}^{N-1} b_j T_j(x).$$

Collocate nonlinear coupling at N Chebyshev points

$$2\sum_{m=1}^{M} a_m \mathrm{se}_m\left(\cos^{-1}(x)\right) \mathrm{Hse}_m(0) = \left[C_1(x) + C_2(x)\left|\sum_{j=0}^{N-1} b_j T_j(x)\right|\right]\left[\sum_{j=0}^{N-1} b_j T_j(x)\right].$$

Collocate kinematic relation at M Chebyshev points

$$\sqrt{1-x^2}\cdot\frac{\partial \phi_{\mathrm{I}}}{\partial y}(x) + \sum_{m=1}^{M} a_m \mathrm{se}_m\left(\cos^{-1}(x)\right) = \sqrt{1-x^2}\cdot C_0(x)\sum_{j=0}^{N-1} b_j T_j(x).$$

BC III: Forchheimer (nonlin. inertial correction for large Re)

Results in nonlinear system:

$$A\mathbf{v} + (B\mathbf{v}) \circ |C\mathbf{v}| = \mathbf{c}$$

$$A = \left(\begin{array}{c|c} A_{11} & A_{12} \\ \hline A_{21} & A_{22} \end{array}\right), B = \left(\begin{array}{c|c} 0 & 0 \\ \hline 0 & B_{22} \end{array}\right), C = \left(\begin{array}{c|c} 0 & 0 \\ \hline 0 & C_{22} \end{array}\right).$$

Decouple via

$$\mathbf{v}_1 = A_{11}^{-1} \left(\mathbf{c}_1 - A_{12}\mathbf{v}_2\right).$$

Solve following via Newton's method:

$$\left[A_{22} - A_{21}A_{11}^{-1}A_{12}\right] \mathbf{v}_2 + (B_{22}\mathbf{v}_2) \circ |C_{22}\mathbf{v}_2| = -A_{21}A_{11}^{-1}\mathbf{c}_1.$$

In all tested cases:

- < 10 iterates needed.
- Initial vector chosen to be solution of linear model.
- Deflation yielded no further solutions.

Typical convergence behaviour

$$C_0(x) = k_0^2, \quad C_1(x) = \mathrm{i}k_0(1.2 + \sin(20x)), \quad C_2(x) = \mathrm{i}20k_0^2(x^2+1),$$

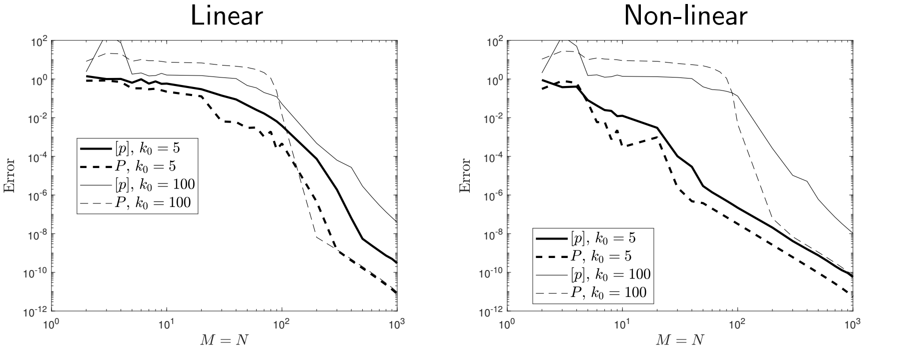

Convergence of the method for the linear case (left) and non-linear case (right).

Application III: Porous foam aerofoils without turbulent sim.

Comparison with Large Eddy Simulations of [Koh et. al. 2018] (quadrupole sound source at trailing edge).

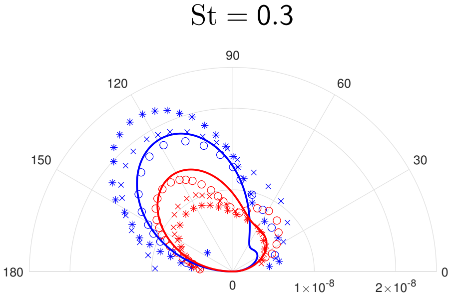

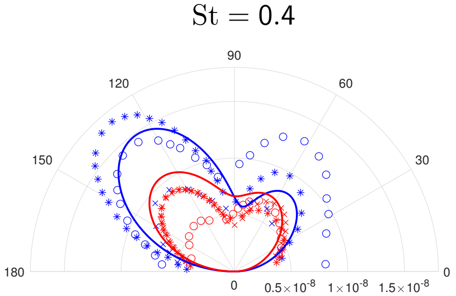

Far-field directivity, LES (symbols) and model (solid). Blue corresponds to impermeable/solid, and red to porous. Data computed in less than 0.1s on six year-old laptop

Concluding Remarks

Numerical:

- This simple and flexible approach works well in different scenarios and applications (low-mid frequency scattering off $\lesssim 100$ plates)
- More accurate and faster than basic BEM (comparison in papers).
- Can "diagonlisation" of SIEs be made more general and automatic?
- Can we cope with different domains, e.g. "V" shaped boundaries?
- Can we make it faster (e.g. sparse methods, hierarchical solvers ...) to deal with > 100 scatterers (e.g. model barbules of owl's wing)?
- How to deal with polylogarithmic singularities more effectively?
- Extension to unbounded plates underway (with A. Hales).

Physical:

(I) Porosity *distributions* important due to destructive interferences.

(II) Acoustic BHs can lead to "transparent" plates and counter-intuitive scattering/sound absorption.

(III) At mid-high k_0 and high permeability, inertial effects can dominate. Inclusion corrects prev. models' over-prediction of noise reduction!

References

BC/Application I:

- M. Colbrook, M. Priddin. “Fast and spectrally accurate numerical methods for perforated screens.” *IMA Journal of Applied Mathematics*, 2020.
- L. Ayton, M. Colbrook, T. Geyer, P. Chaitanya, E. Sarradj. “Reducing aerofoil–turbulence interaction noise through chordwise-varying porosity” *Journal of Fluid Mechanics*, 2020.

BC/Application II:

- M. Colbrook, A. Kisil. “A Mathieu function boundary spectral method for scattering by multiple variable poro-elastic plates, with applications to metamaterials and acoustics.” *Proc. Royal Society A*, 2020.

BC/Application III:

- M. Colbrook, L. Ayton. “Do we need non-linear corrections? – On the boundary Forchheimer equation in acoustic scattering.” *Journal of Sound and Vibration*, under review.

If you have suggestions or problems for collaboration, please get in touch!

Quadrupole at $(x, y) = (-1, 0.001)$, $k_0 = 25$, $h(x) = 0.001(x+1)^2 + h_0$

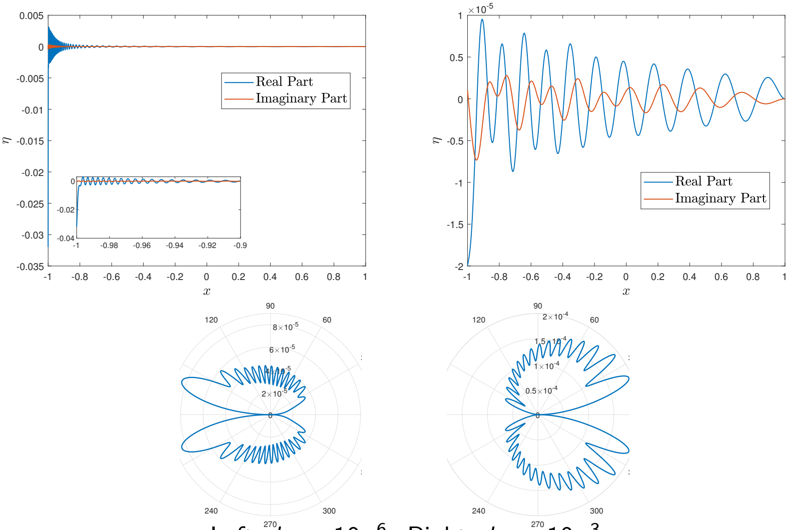

Left: $h_0 = 10^{-6}$. Right: $h_0 = 10^{-3}$.

Comparison with BEM

Compare with *Cavalieri, Wolf, & Jaworski, "Numerical solution of acoustic scattering by finite perforated elastic plates"*, *Proceedings A 2016*.

Uses BEM method with basis functions constructed using vibration modes of the plate (computed using standard spectral methods).

$$(1-\alpha_H)\frac{\partial^4\eta}{\partial x^4} - \frac{k_0^4}{\Omega^4}\eta = -\left(1+\frac{4\alpha_H}{\pi}\right)\frac{\epsilon}{\Omega^6}k_0^3[\phi],$$
$$\frac{\partial\phi}{\partial y}\Big|_{y=0} + \frac{\partial\phi_{\mathrm{I}}}{\partial y}\Big|_{y=0} = (1-\alpha_H)k_0^2\eta + \frac{2\alpha_H}{\pi R}[\phi].$$

<u>Constant</u> parameters:
Ω = vacuum bending wave Mach number
$\epsilon = 0.0021$ = fluid-loading

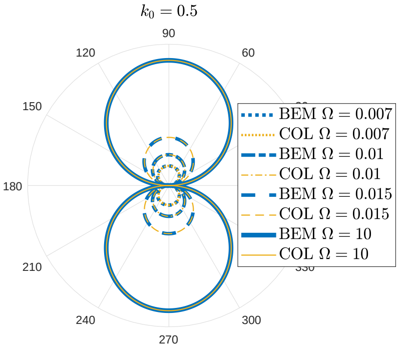

$k_0 = 0.5$
90
60
120
150
180
210
240
270
300
330
BEM $\Omega = 0.007$
COL $\Omega = 0.007$
BEM $\Omega = 0.01$
COL $\Omega = 0.01$
BEM $\Omega = 0.015$
COL $\Omega = 0.015$
BEM $\Omega = 10$
COL $\Omega = 10$
$k_0 = 20$
BEM $\Omega = 0.05$
COL $\Omega = 0.05$
BEM $\Omega = 0.06$
COL $\Omega = 0.06$
BEM $\Omega = 0.1$
COL $\Omega = 0.1$
BEM $\Omega = 1000$
COL $\Omega = 1000$

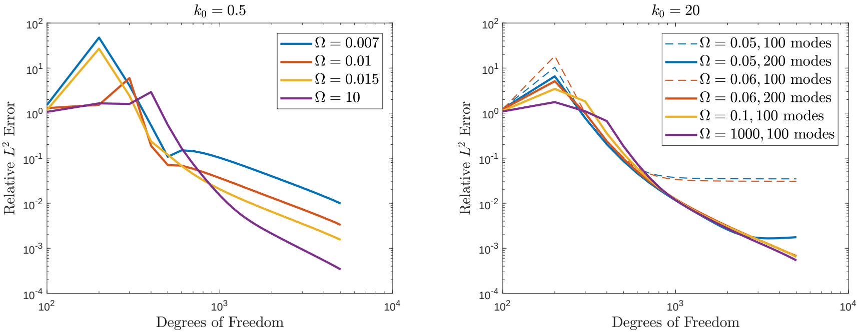

Left: Convergence of elastic BEM for $k_0 = 0.5$ (100 modes). Right: Same but for $k_0 = 20$ (number of modes shown).

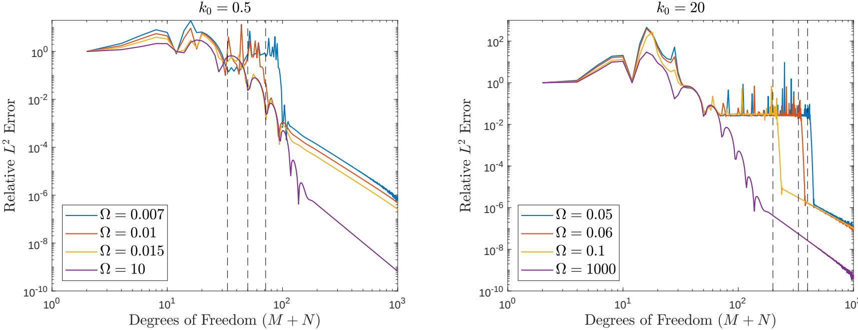

Left: Convergence of Mathieu function collocation for $k_0 = 0.5$. The vertical dashed lines are positioned at the bending wavenumbers $k_B = k_0/\Omega$ (too small to plot for $\Omega = 10$). Right: Same but for $k_0 = 20$.

Case	Material	Ref. (see [C. & Ayton 2020])
1	Impermeable	-
2	Alantum NiCrAl open-cell metal foam	[Rubio et. al. 2019]
3	Sintered PE granulate (Porex)	[Geyer et. al. 2014]
4	Sintered SUS316L powder (Group 2, 9mm)	[Zhong et. al. 2018]

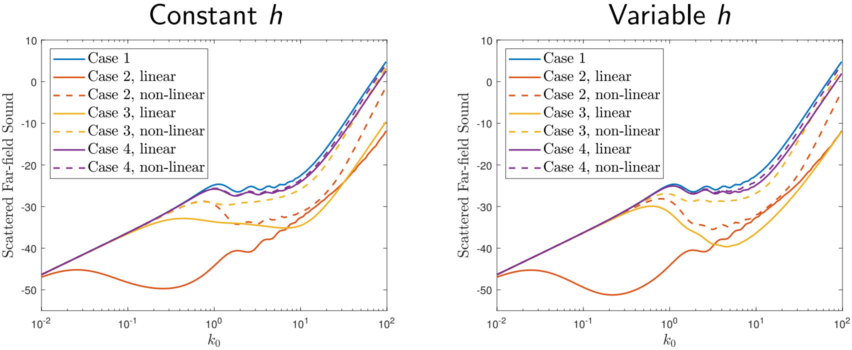

Far-field sound. Left: Results for non-dimensionalised thickness of $h(x) = 0.012$. Right: Results for an NACA 4-digit aerofoil.